Electronic Supplementary Material (ESI) for Journal of Materials Chemistry C.

Supplemental Material

Magnetoresistance of High Mobility HgTe Quantum Dot Films with Controlled Charging

Menglu Chen, Xinzheng Lan, Margaret H. Hudson, Guohua Shen, Peter B. Littlewood, Dmitri V. Talapin, Philippe Guyot-Sionnest**

1. TEM of different size HgTe CQD

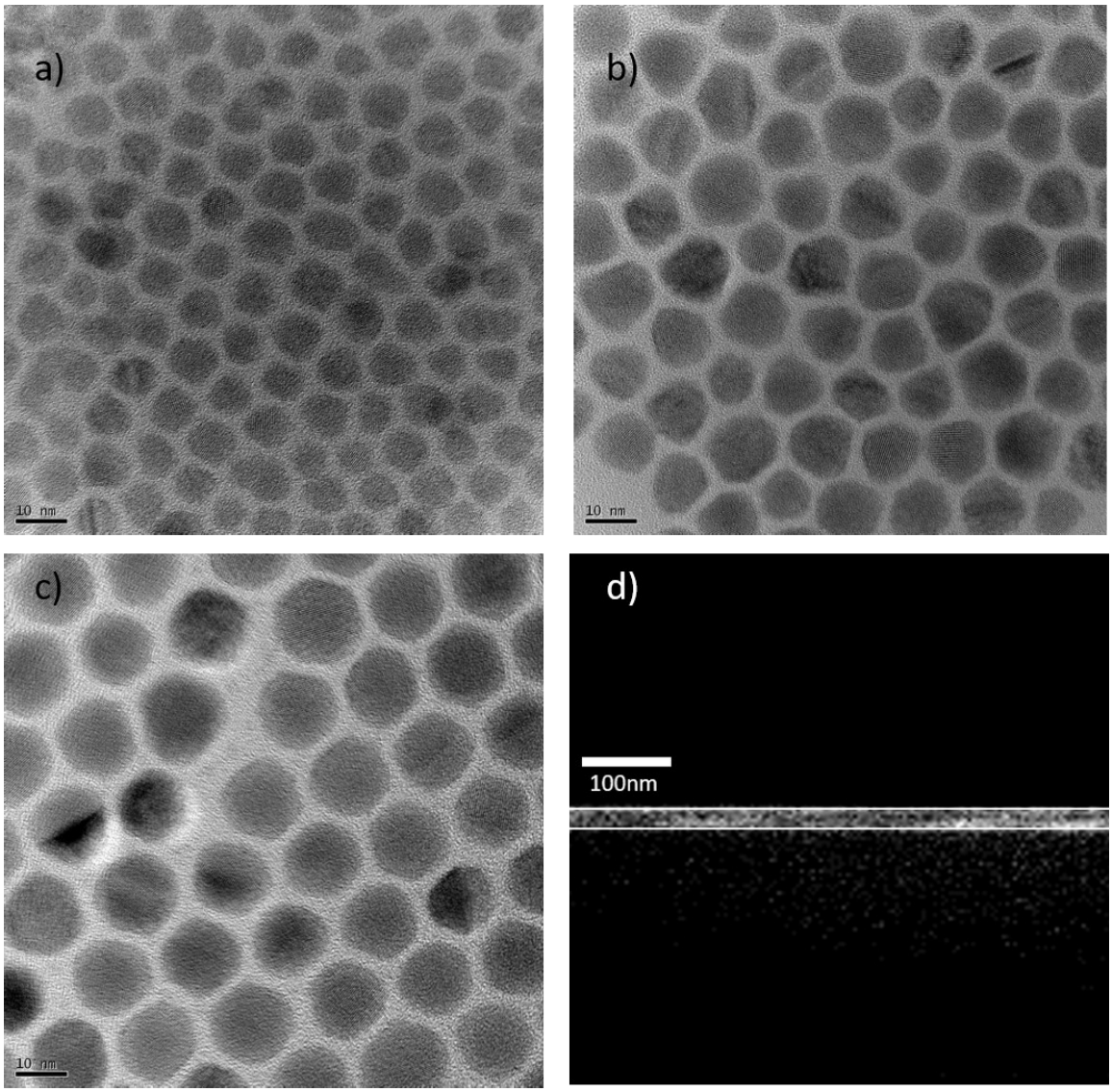

Figure S1. a)b)c)TEM of 8.0 ±1.0 nm , 11.5 ±1.3 nm and 15.0nm ±1.2 nm diameter HgTe CQD, respectively. d) SEM. Cross section of 11.5nm diameter HgTe CQD, ~2 layers.

2. Comparison between self doping and solid state gating

Figure S2a shows FET curve with different self-doping level (~1e/dot) or without (~0.2e/dot). Figure S2b shows one example on MR curve at 50K for 15 nm diameter HgTe with 1Se state half-filled achieved by self-doping (black) or FET gating (grey). With MR measurement with FET gating, one needs to be more careful about the bias applied. The different bias between source and gate and drain and gate induces carrier number differences between source and drain. Fig S2c shows that with a small bias, there is no obvious positive or negative source-drain bias effect on MR while a large bias causes an artificial effect on MR. The source-drain bias does not affect the MR of self-doped CQD films at 0V gate bias. For this reason, in the FET measurement with magnetic field, we only used a small bias of ~0.1V.

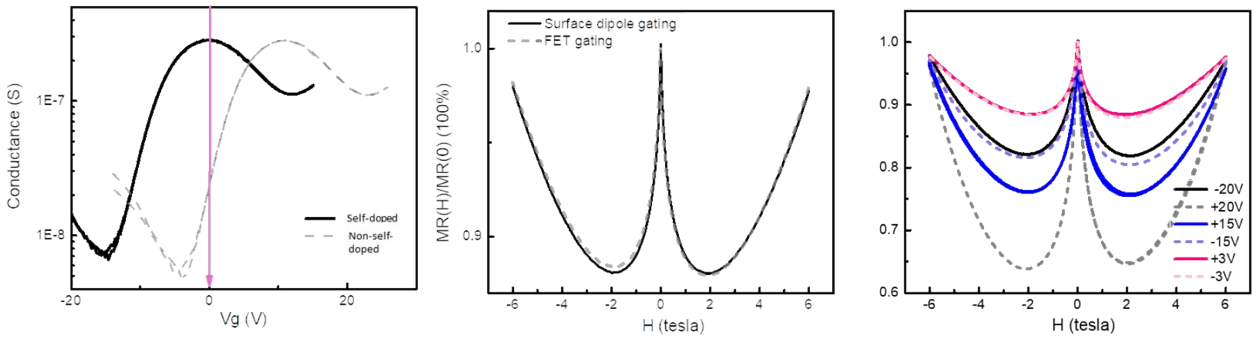

Figure S2. comparison between samples with self-doping of ~ 1 e^-/dot and 0.2 e^-/dot. a) FET curve of 15nm diameter HgTe self-doped (black) or non-self-doped (grey) at 50K. b) MR curve at 50K at 1 e^-/dot for two samples of 15 nm diameter HgTe. The solid line is for a sample that is self-doped so that 1e^-/dot so that the gate bias is 0V. The dashed line is for a sample that is self-doped with 0.2e-dot and the gate bias is 12V while the source-drain bias is 1.5V. c) Effect of source-drain bias on the MR of a FET gated sample at a fixed gate voltage.

3. 8nm diameter HgTe CQD solid MR

Figure S3 shows the MR of 8nm diameter HgTe CQD solid at 100K and 20K. The film thickness is ~60nm (around 8 layers quantum dots). The MR could also be fitted nicely by the equation mentioned in the main text with $g \sim 70$.

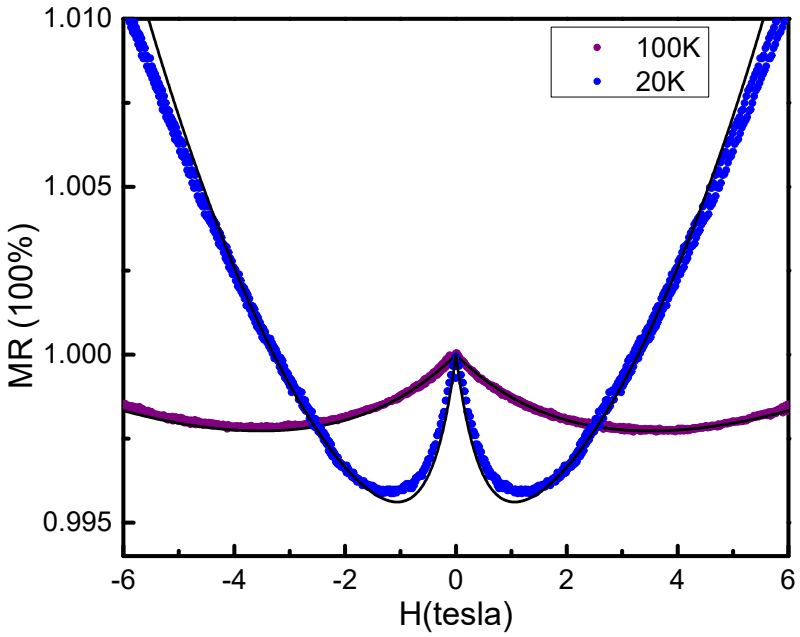

Figure S3. MR for a 8nm diameter HgTe CQD solid.

4. Substrate and electrode effect on MR.

Substrate and electrode material have no obvious effect on MR. Figure S6 shows the MR curve measured with different substrate and electrode. The MR curves almost overlap, indicating that the resistance change does not come from the substrates or electrodes and that the MR is robust and very repeatable. Changing the film area from 3mm x 1mm to 3mm x 5μm also has no obvious effect on the MR.

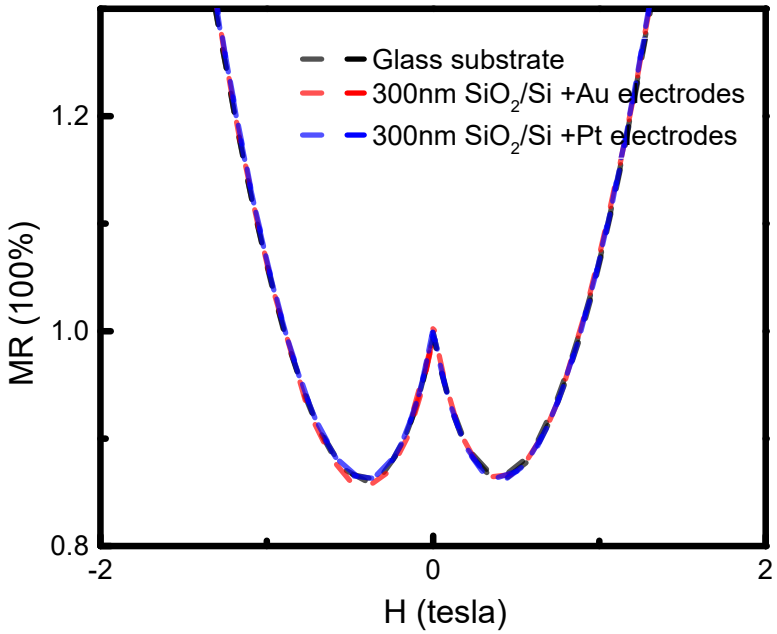

Figure S4. MR of 15nm diameter HgTe CQD at 10K with different substrate and electrode.

5. Low mobility HgTe MR

EDT treated HgTe solids have 2 order of magnitude smaller mobility compared to polar ligands HgTe solids. The MR, however, has similar behaviors. Figure S8 shows the MR at 50K of low mobility and high mobility 11.5nm HgTe CQD film with similar thickness.

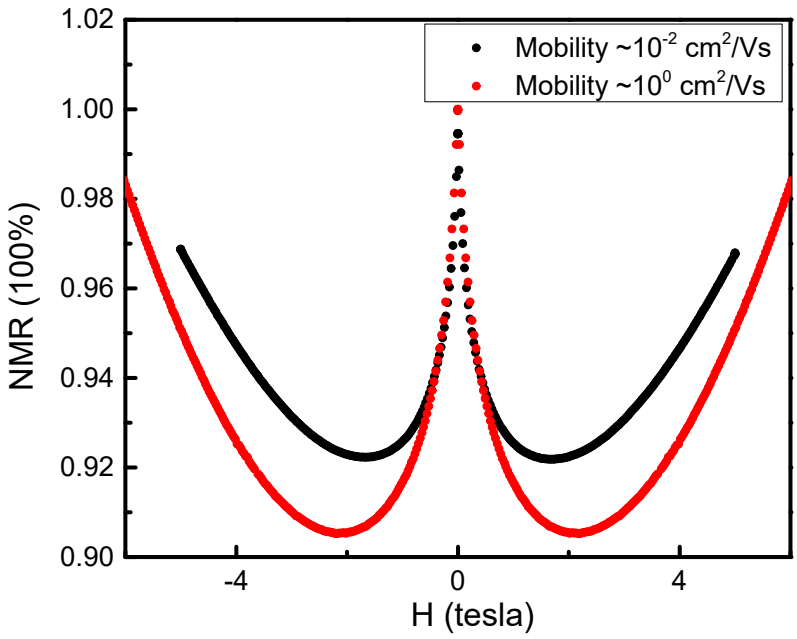

Figure S5. MR on low mobility (Black curve) and high mobility (red curve) 11.5 nm diameter HgTe CQD films at 50K.

6. Estimation of effective mass

The K•P model gives the energy dispersion $E = \frac{1}{2}\left(\frac{\hbar^2 k^2}{m_0} - E_g\right) + \sqrt{\frac{\hbar^2 k^2}{2m_0}E_p + \frac{E_g^2}{4}}$. The effective mass of electron at $1S_e$ state could be given by

$$\frac{1}{m^*} = \frac{\partial^2 E}{\hbar^2 \partial k^2} = \frac{1}{m_0} + \frac{E_p}{2m_0}\frac{1}{\left(\frac{\hbar^2 k^2}{2m_0}E_p + \frac{E_g^2}{4}\right)^{1/2}} - \frac{\frac{\hbar^2 k^2}{4{m_0}^2}{E_p}^2}{\left(\frac{\hbar^2 k^2}{2m_0}E_p + \frac{E_g^2}{4}\right)^{3/2}}$$

Where k=π/R for $1S_e$ (R=7.5nm in our case), energy gap E_g =-0.2eV. E_p is the Kane parameter E_p=18eV (typical for II-VI and III-V semiconductors), giving $m^* = 0.04m_0$ while E_p = 9 eV (better fit of the size tuning of the HgTe CQDs), giving $m^* = 0.025m_0$.

7. Optical measurement.

A independent measurement on g would be helpful to confirm the value of g used to fit the MR. We attempted such measurements but without conclusive evidence due to limited sensitivity and the lack of a strong enough magnetic field.

$\mathcal{g}$ here is noted as the total angular momentum (Landé) $\mathcal{g}$-factor. With $\mathcal{g}$~100 and a permanent magnet with 0.5 T magnetic field, the Zeeman shift would be 10cm^{-1} and accessible by FTIR spectroscopy. The sensitivity is limited for the following reasons. First, considering all the possible $1S_e$-P_e transitions shown in FigureS10a, the average peak position would not change but only the broadening would increase, and only if g is different for $1S_e$ and $1P_e$. Second, the experimental lines are much broader than the calculated shift. In this case, the convolution(Voigt) of homogenous broadening (Lorentzian) and inhomogeneous broadening (Gaussian) reduces the visibility of the broadening as shown in Figure S10b, which shows a simulation of Voigt spectra with a fixed inhomogeneous (200cm^{-1}) and homogenous (400cm^{-1}) before and after the homogeneous line is split in two lines with 10cm^{-1} separation（red 410cm^{-1} ， green 400cm^{-1} ）. The insert graph shows that the splitting has essentially no effect, except down in the wings. However, this is where it is hard to measure by FTIR absorption because of the background level. Figure S10c shows the experimental intraband absorption with/without external magnetic field (0.5tesla) of 11.5nm HgTe CQD. A 10T magnetic field should easily lead to spectroscopic effects

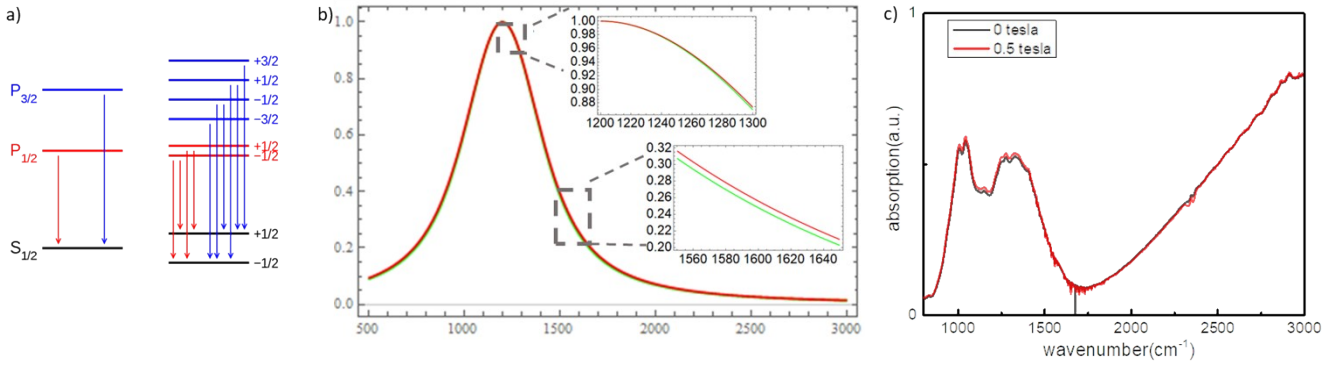

given the small linewidth of the $1S_{e1/2}$-$1P_{e1/2}$ transition around 1000cm^{-1}.

Figure S6. a) Possible transition for S-P state. b) simulation of Voigt with different homogenous broadening. c) Intraband absorption with/without external magnetic field of 11.5nm HgTe CQD.